Combined NMR–crystallographic and modelling investigation of the inclusion of molsidomine into α–, β– and γ–cyclodextrins

ARTICLE *in* BIOORGANIC & MEDICINAL CHEMISTRY · JANUARY 2006

Impact Factor: 2.79 · DOI: 10.1016/j.bmc.2005.07.009 · Source: PubMed

5 AUTHORS, INCLUDING:

Gloria Uccello-Barretta
Università di Pisa
156 PUBLICATIONS **2,018** CITATIONS
SEE PROFILE

Federica Balzano
Università di Pisa
93 PUBLICATIONS **983** CITATIONS
SEE PROFILE

Donatella Paolino
Universita' degli Studi "Magna Græcia" di C…
98 PUBLICATIONS **2,069** CITATIONS
SEE PROFILE

Available online at www.sciencedirect.com
SCIENCE DIRECT®
Bioorganic & Medicinal Chemistry 13 (2005) 6502–6512
Bioorganic & Medicinal Chemistry

Combined NMR-crystallographic and modelling investigation of the inclusion of molsidomine into α-, β- and γ-cyclodextrins

Gloria Uccello-Barretta,[a,*] Federica Balzano,[a] Donatella Paolino,[b,†] Rebecca Ciaccio[b] and Salvatore Guccione[b,*]

[a]*Dipartimento di Chimica e Chimica Industriale, Università degli Studi di Pisa, via Risorgimento 35, 56126 Pisa, Italy*
[b]*Dipartimento di Scienze Farmaceutiche, Università degli Studi di Catania, V.le A. Doria 6, Ed. 2 Città Universitaria, I-95125 Catania, Italy*

Received 18 December 2004; revised 4 July 2005; accepted 4 July 2005
Available online 16 September 2005

Abstract—A NMR spectroscopic and crystallographic investigation supported by molecular modelling methods has been employed to describe the inclusion properties of molsidomine into the three underivatized α-, β- and γ-cyclodextrins, aimed to point out the factors affecting the complexation selectivity and stabilization. The NMR results were compared and validated by the analysis of crystallographic data as retrieved from the Cambridge Structural Database and molecular modelling studies.

1. Introduction

Cardiovascular disease (CVD) refers to a group of disorders of the heart and blood vessels that include hypertension, congestive heart failure, heart attack, stroke, coronary artery disease, angina, atherosclerosis, rheumatic heart disease and congenital heart disease. According to WHO estimates, 16.7 million people around the globe die of cardiovascular diseases each year. CVD is the leading cause of death in the European Union, accounting for over 1.5 million deaths each year.[1]

Angina is a pain or discomfort in the chest or adjacent areas caused by insufficient blood flow to the heart muscle. Angina, also called angina pectoris, is a symptom of ischemic heart disease (IHD). Chest pain, pressure and discomfort—commonly known as angina—result when the coronary arteries do not deliver an adequate amount of oxygen-rich blood to the heart (called ischemia).[1,2a,b]

Research over the past 20 years has identified endogenous nitric oxide (NO) as a key messenger molecule in the cardiovascular, nervous and immune systems. Delivery of exogenous NO is an attractive therapeutic option in the treatment of cardiovascular disease. Organic nitrates were first used to relieve the symptoms of angina over a century ago, long before the identification of NO as an endogenous messenger. It is now recognized that the beneficial effects of organic nitrates are mediated by NO and, despite limitations, they remain the most commonly used NO donor drugs in cardiovascular medicine.[2a,b,3–6] Multifunctional nitric oxide releasing morpholine derivatives with antioxidant, hypolipidemic and NO-releasing potential that could favour the inhibition of the major atherogenic mechanisms have been recently reported.[7]

Nitrates dilate blood vessels through the NO–sGC (soluble Guanylate Cyclase) mechanism. Although nitrates can dilate coronary arteries, they are recognized to be venoselective and their effects are primarily mediated by reduced venous return and the consequent reduction in cardiac workload. Molsidomine (3-morpholine-sydnoneimine) is the endogenous precursor of the NO donor, 3-morpholinosydnonomine (SIN-1) (Fig. 1), which has been shown to stimulate sGC activity by an NO-mediated pathway in blood vessels. Conversion of molsidomine to SIN-1 occurs primarily in the liver in vivo and subsequent transformation of SIN-1 to SIN-1A occurs

Keywords: Combined investigation; Molsidomine; Complexes; Inclusion selectivity; Cyclodextrins; NMR; DOSY.
* Corresponding authors. Tel.: +39 0502219232; fax: +39 0502219260 (G.U.-B.); tel.: +39 095 738 4020; fax: +39 095 443604 (S.G.); e-mail addresses: gub@dcci.unipi.it; guccione@unict.it
† Present address: Dipartimento di Scienze Farmacobiologiche, University Magna Graecia Catanzaro, Complesso Ninì Barbieri, I-88021 Roccelletta di Borgia (CZ), Italy.

0968-0896/$ - see front matter © 2005 Elsevier Ltd. All rights reserved.
doi:10.1016/j.bmc.2005.07.009

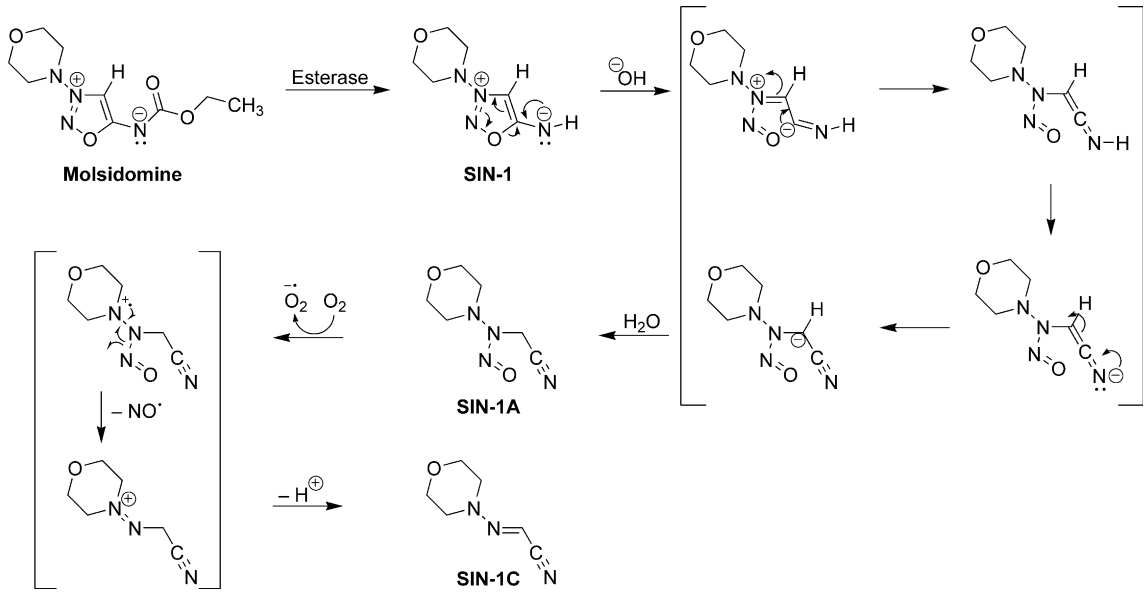

Figure 1. Activation mechanism of molsidomine.[2]

spontaneously in the blood via a hydrolytic cleavage. Molecular oxygen initiates conversion of SIN-1A to SIN-1C, resulting in the release of NO (Fig. 1), a reaction that is accelerated by O_2. Formation of *S*-nitrosoglutathione has also been implicated as an intermediary step prior to activation of sGC.[2a,b,3–6]

The beneficial effects of molsidomine were recognized before endogenous NO was identified and were first applied in the treatment of angina in 1978.[2a,b,6] However, the mechanism by which molsidomine and SIN-1 cause vascular relaxation and inhibit platelet activation is a controversial issue because, although the effects of these compounds are associated with increased cGMP, there is a poor correlation between both the time course and extent of cGMP elevation and the observed hemodynamic effect. A possible explanation may revolve around activation of K^+ channels. Molsidomine has a slower onset and longer duration of action than conventional nitrates due to the relatively slow rate of conversion to SIN-1. SIN-1 itself has a rapid onset and short duration of action. Interestingly, molsidomine and SIN-1 do not appear to induce tolerance, and are not cross-tolerant with conventional nitrates. Molsidomine and SIN-1 are therapeutic alternatives to traditional organic nitrates in stable angina, coronary vasospasm and heart failure, with the obvious benefit of avoiding tolerance.[2a,b,3–8]

To optimize the efficacy of molsidomine activity through the use of rationally designed drug carrier materials, its release behavior from alcanoylated cyclodextrin complexes has been previously discussed.[9]

In fact, cyclodextrins constitute a family of truncated, cone-shaped cyclic oligosaccharides, among which the most common systems are constituted by six (α-CD), seven (β-CD), or eight (γ-CD) glucopyranose rings. Their most popular feature is the marked difference of polarity between the internal and external surfaces: the inner part is made apolar by the glycosidic oxygens

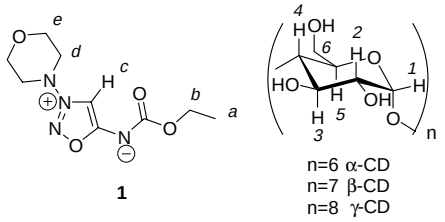

Figure 2. Molsidomine (**1**), α-CD, β-CD and γ-CD.

and methine protons, whereas the external surface is polar by virtue of the presence of secondary and primary hydroxyls on the large and small rims, respectively, thus allowing their solubilization in water. These unique properties predispose them to form inclusion complexes, as the displacement of included water molecules by apolar substrates represents a thermodynamically favoured process.[10] Their ability to act as hosts in the formation of inclusion complexes has also been extensively exploited in their use as release drug carriers to improve the physicochemical and pharmaceutical properties of the administered molecules.[10]

We describe now the results of our NMR investigation on the inclusion properties of molsidomine (**1**) into the three underivatized cyclodextrins (Fig. 2), aimed to point out the factors affecting the complexation selectivity and stabilization. The NMR results are compared and validated by the analysis of crystallographic data as retrieved from the Cambridge Structural Database (CSD)[11a–c,12a,b] (version 5.25, November 2003; data update 3: July 2004) and molecular modelling studies.

2. Results and discussion

2.1. NMR investigations

The ^1H NMR (600 MHz) spectrum of molsidomine (20 mM) in D_2O shows well resolved signals in three

distinct spectral regions: a sharp triplet centered at 1.13 ppm due to the methyl nuclei H-a, which are J-coupled to the adjacent methylene protons H-b, giving a quartet at 4.02 ppm (Fig. 3A).

At 3.88 ppm and 3.52 ppm are found two multiplets (Fig. 3A), each integrating for four protons, and respectively corresponding to the two pairs of equivalent methylene protons of the morpholine ring adjacent to the oxygen (H-e) and nitrogen (H-d) nuclei. In the high frequency region, the sharp singlet (7.88 ppm) due to the H-c proton is clearly detected. The presence of equimolar amounts of every cyclodextrin caused detectable complexation shifts of molsidomine protons ($\Delta\delta = \delta_{mix} - \delta_{free}$, δ_{mix} chemical shift measured in the mixture and δ_{free} chemical shift of the free compound). The origin of these effects has been ascertained by comparing the association constants of the three complexes by Diffusion-Ordered SpectroscopY (DOSY) techniques and by determining their stereochemical features by means of monodimensional ROESY analyses.

2.1.1. Analysis of the complexation shifts. The ^{1}H NMR spectra of pure molsidomine and its equimolar mixtures with α-CD, β-CD and γ-CD are compared in Figure 3, whereas Figures 4–6 report the proton spectra of every mixture together with those of the pure hosts.

The entities of the complexation shifts measured in the three mixtures (Table 1) can be analyzed separately but not compared to each other, as in principle, these could be originated by complexes where molsidomine is included with different relative stereochemistry.

α-Cyclodextrin very much affected the side chain ethyl protons of molsidomine and its H-c proton, in fact complexation shifts of 34.6, 14.3 and −17.2 Hz were, respectively, measured (Table 1). Therefore, the ethyl group of the drug should be involved in the complexation with the cyclodextrin. Significantly, minor effects were detected on the morpholine protons (Table 1). The analysis of the variations undergone by cyclodextrin protons as a consequence of the presence of molsidomine strongly suggests complexation involving inclusion into the

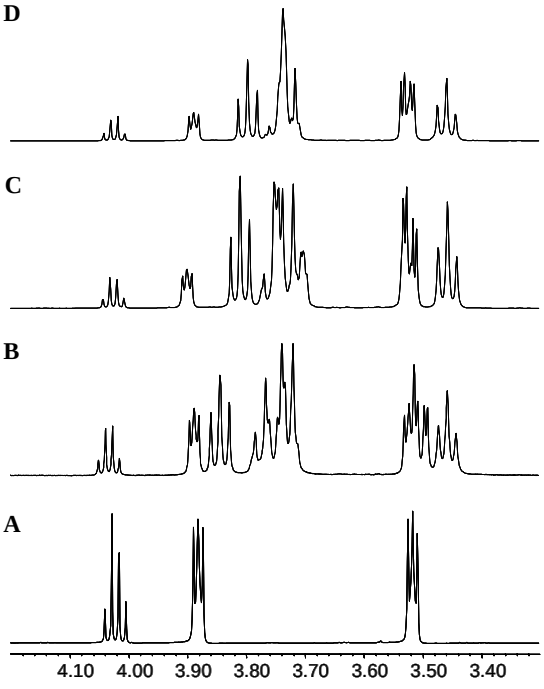

Figure 3. ^{1}H NMR (600 MHz, D_2O, 25 °C) spectral regions including the methylene protons of (A) **1** (total concentration 20 mM), (B) the 1:1 mixture α-CD/**1** (total concentration 40 mM), (C) the 1:1 mixture β-CD/**1** (total concentration 31.8 mM) and (D) the 1:1 mixture γ-CD/**1** (total concentration 40 mM).

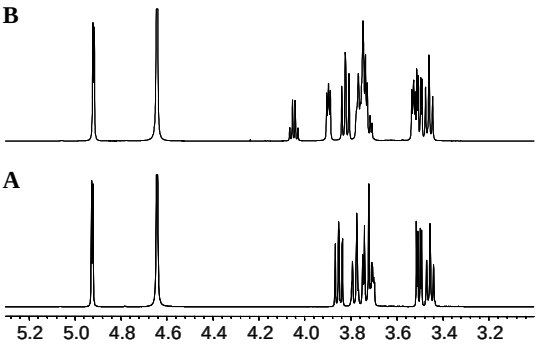

Figure 4. ^{1}H NMR (600 MHz, D_2O, 25 °C) spectral regions including the CD resonances of (A) α-CD (20 mM) and (B) 1:1 mixture α-CD/**1**.

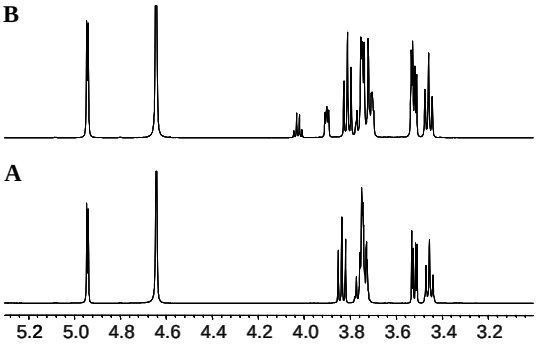

Figure 5. ^{1}H NMR (600 MHz, D_2O, 25 °C) spectral regions including the CD resonances of (A) β-CD (15.9 mM) and (B) 1:1 mixture β-CD/**1**.

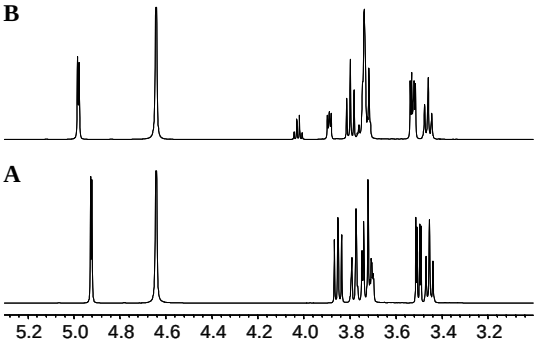

Figure 6. ^{1}H NMR (600 MHz, D_2O, 25 °C) spectral regions including the CD resonances of (A) γ-CD (20 mM) and (B) 1:1 mixture γ-CD/**1**.

Table 1. Complexation shifts ($\Delta\delta$) data (600 MHz, D_2O, 25 °C) of mixtures obtained starting from **1** (20 mM) and one equivalent of α-, β- and γ-CD

	$\Delta\delta = \delta_{mix} - \delta_{free}$ (Hz)		
	α-CD/**1**	β-CD/**1**[a]	γ-CD/**1**
***1** Protons*			
H-a	34.6	3.4	6.8
H-b	14.3	1.0	1.0
H-c	−17.2	−19.9	−10.5
H-d	5.1	5.1	4.4
H-e	8.2	10.5	4.6
CD protons			
H-1	−3.1	0	−1.4
H-2	−1.3	1.4	0.3
H-3	−26.7	−14.8	−4.7
H-4	2.5	2.0	−0.7

[a] Measured at 15.9 mM due to the β-CD solubility.

cavity of the host, as the external protons H-1, H-2 and H-4 were slightly affected, whereas the internal H-3 protons located on the internal large rim show a complexation shift of −26.7 Hz. Unfortunately, the extensive superimposition between some cyclodextrin resonances enabled us to obtain precise values of the complexation shifts of the internal H-5 protons or of the external H-6 protons, which could have been decisive to establish if the inclusion occurs by the large diameter rim or by the small one. Anyway, as we will show later, this problem has been completely overcome by analysis of the intermolecular NOEs.

An analogous analysis of the complexation shifts of molsidomine due to β-CD revealed a different trend (Table 1): the chemical shifts of morpholine protons underwent variations till 10.5 Hz, the variation observed for the proton Hc was analogous to that found in the presence of the smaller oligosaccharide, being −19.9 Hz, and lower effects were produced in the ethyl protons. On this basis, a preference for the complexation of the morpholine moiety could be hypothesized. The complexation involves once again inclusion as the external protons of cyclodextrin are significantly less affected relatively to the H-3 internal protons (Table 1). Also in this case, no decisive conclusions can be drawn about the stereochemistry of the inclusion into the cavity.

The interaction between the drug and γ-CD seems to involve copresence of complexed forms in which molsidomine is included by both its ethyl and morpholine moieties. In fact, comparable complexation shifts were measured for the protons corresponding to the two moieties, besides a prevalent effect on the H-c proton; internal protons of the cyclodextrin felt effects more relevant than external ones (Table 1).

Therefore, on the basis of the simple analysis of complexation shifts, some differences of the selectivity of the inclusion into the three cyclodextrins can be pointed out: α-CD shows a marked preference for the inclusion of the ethyl group of molsidomine, β-CD seems to include preferentially the morpholine ring, whereas γ-CD does not show any preference for the inclusion of one group with respect to the other. The common feature is the strong involvement of the sydnone moiety in the interaction with every cyclodextrin, as it undergoes always the more relevant complexation shifts. Competing *shuttle systems* to direct the inclusion of the morpholine and ethyl fragments, respectively, by binding to polar exosites in the cyclodextrin molecule can be supposed with the positively charged N3 on one side and the pair exocyclic imine-N and carbonyl ester O53 on the other side, acting as anchor points. The exocyclic imine-N and the carbonyl ester O13 might act as a *two-pronged* feature complementing each other opposite to the above mentioned positive N as carrier of the morpholine ring inclusion.

The larger β- and γ-cyclodextrins could be able to accommodate the chair morpholine ring and both the morpholine and ethyl groups, respectively. A similar length oriented spatial disposition of the piperazine ring allows to compensate for the steric hindrance and led to a favourable interaction of some dopamine antagonists, whereas alkyl derivatives ($n > 2$) *width* oriented in the space are inactive.[13] Considering the crystal packing[12a,12b] once inside the cavity, lots of shorter contacts might be involved in the stability of the host–guest complex (Fig. 7).

The process might finally be governed by steric factors, in the case of the α-cyclodextrin due to the chair length oriented shape of the morpholine ring which cannot be located into the smaller α-cyclodextrin. According to the crystal structure where the exocyclic imine-N51 and the O53 form two independent H bonds with water molecules (Fig. 7), a synergy by these two groups might be the driving force, mainly leading to the ethyl fragment inclusion with the above two water molecules at the same time or alternatively replaced by the polar groups in the external part of the cyclodextrin.

According to the molsidomine X-ray structure[12a,12b], water molecules might be important to stabilize the molecule conformation in terms of solvation energy, as also

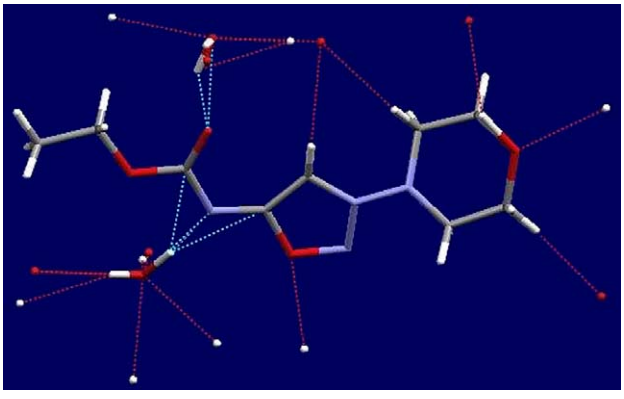

Figure 7. Key intermolecular interactions of the molsidomine crystal structure CSD (version 5.25, November 2003. Data update 3: July 2004. Code: KABZES), with bound water molecules to Carbonyl O53 and Imine nitrogen N51 as in the crystal packing. The hydrogen bonds are shown as broken blue lines. Other short contacts are shown as broken red lines. Numbering scheme according to Ref. 12a.

the conformational analysis by the software MACROMODEL (version 8.1)[14a–c] proved (GB/SA model). The best fitting *aqueous* conformer (RMSD 0.319 Å) to the X-ray structure when alone used as the starting structure is located at a value above the minimum (-81.33 kJ mol^{-1}) of about 12 kJ mol^{-1}. The actual lowest energy conformer shows an opposite spatial disposition of the N(51)-C(56) side chain moiety with respect to the crystal structure (RMSD 0.7475 Å). A quite similar result was obtained starting from a de novo built structure using the MACROMODEL (version 8.1) fragment library[14a–c] with the N(51)-C(56) fragment pointing *down* from the molecular plane contrary to that *up* in the X-ray structure. The higher RMSD value was due to the opposite N(51)-C(56) side chain moiety position retained also in the lowest energy conformer (Fig. 8). No differences were in the conformational analysis using the TORS command (atoms 13–15 and the whole molecule) instead of the TORC command which is assigned as a default in amides and puts limits on the values of the torsions for N–C bonds. The same result was obtained including the two bound waters (MOLS command automatically *on*) as in the X-ray structure in the conformational search, but the conformers found were lower in energy when compared to the above GB/SA model where the missing generation of restraints by the water molecules does not lead to 'alternate' more stable conformations. One (#2481) out of the 3903 conformers found including the two water molecules at 11.64 kJ (-161.62 kJ mol^{-1}) higher than the minimum (-173.26 kJ mol^{-1}) reproduced the experimental situation with the two waters which stay in about the same position as in the X-ray structure.[12a,b] Although the higher energies might indicate a lower performance of the software, a similar trend (the conformer resembling the experimental was found at -19.96 kJ mol^{-1}) with the minimum at -30.68 kJ mol^{-1} was observed freezing the two water molecules (ATOM FREEZE command).[14a,b]

The lowest energy minimum and that 'X-ray mimicry' about 12 kJ mol^{-1} above it did not undergo changes after molecular dynamics.

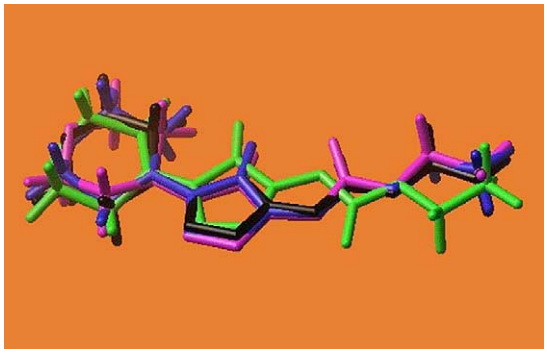

Figure 8. Superposition (non-H atoms superposition alignment and sequence) of the crystallographic (black) and its lowest energy conformers in vacuo (purple: RMSD 0.2903 Å) and aqueous (green: RMSD 0.7475 Å). A quasi theoretical RMSD was obtained with an *aqueous* conformer (blue) at about 12 kJ mol^{-1} above the minimum. No boat conformations of the morpholine were detected (only a more or less distorted ring).

Molecular dynamics with simulated annealing by the software SYBYL 6.9 using the TRIPOS force field[15] showed a substantially similar trend with superimposable conformers (rms deviation 0.6 ÷ 0.8 Å) above the minimum and the tendency for the N(51)-C(56) side chain to rapidly interconvert up–down the molecular plane in the investigation range of 20 kcal mol^{-1} above the minimum.

2.1.2. NOE determinations. To have a complete picture of the above inclusion phenomena, we must define the inclusion stereochemistry of molsidomine. The answer to this question comes from the analysis of the intermolecular NOEs detected in the three mixtures by 1D ROESY analysis (Figs. 9, 10).

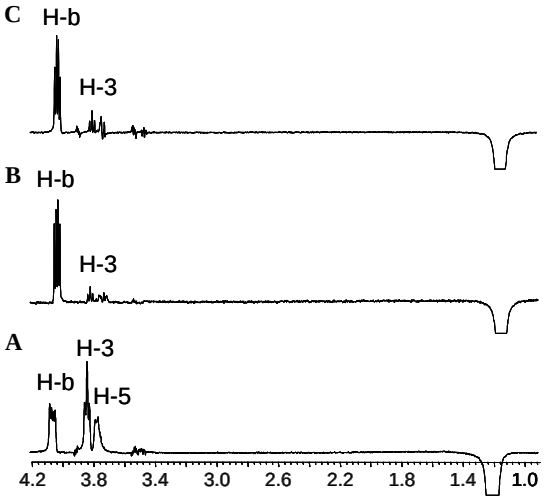

Figure 9. 1D ROESY (600 MHz, D_2O, 25 °C, mix = 1.2 s) spectra corresponding to the selective irradiation of H-a protons of **1** in (A) 1:1 mixture α-CD/**1** (total concentration 40 mM), (B) 1:1 mixture β-CD/**1** (total concentration 31.8 mM) and (C) 1:1 mixture γ-CD/**1** (total concentration 40 mM).

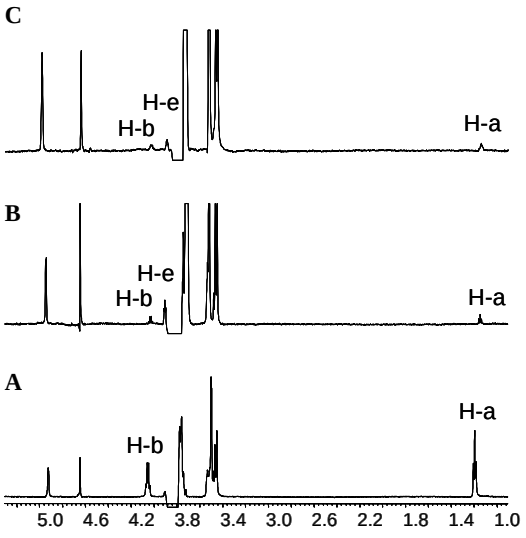

Figure 10. 1D ROESY (600 MHz, D_2O, 25 °C, mix = 1.2 s) spectra corresponding to the selective irradiation of H-3 protons of the cyclodextrin in (A) 1:1 mixture α-CD/**1** (total concentration 40 mM), (B) 1:1 mixture β-CD/**1** (total concentration 31.8 mM) and (C) 1:1 mixture γ-CD/**1** (total concentration 40 mM).

In fact, in the three mixtures, molsidomine protons belonging to the ethyl group (Fig. 9) or morpholine ring, produced larger NOEs on the H-3 protons, located in the larger diameter internal part, than they did on the other internal H-5 protons nearer the smaller diameter rim. Therefore, molsidomine is always included by the larger diameter cavity.

The analysis of the dipolar interactions generated by the internal H-3 protons of the three cyclodextrins (Fig. 10) not only confirmed some features already evidenced by the analysis of the complexation shifts, but also revealed some additional aspects. As a matter of fact, H-3 protons of α-CD produced remarkably intense NOEs on molsidomine ethyl moiety (Fig. 10A), which unequivocally confirms the inclusion of the drug by this group. The NOEs detected on perturbation of the H-3 protons of the other two cyclodextrins are remarkably lower (Figs. 10B and C).

This could indicate a minor degree of complexation produced by significantly smaller association constants with respect to the previous case, which could be consequent to a worse fit between the cavity size and the included moieties. Furthermore, the H-3 protons of β-CD produced NOEs both on morpholine and ethyl protons of the drug (Fig. 10B), but the first were prevailing on the latter, to indicate that in this case the group preferentially included is the morpholine ring, but anywhere else, the inclusion of the ethyl group must be simultaneously taken into account. The H-3 protons of γ-CD determined themselves lower NOEs (Fig. 10C) which were of quite similar intensities for the morpholine and ethyl moieties; therefore the inclusion seems to be scarcely selective.

It is noteworthy that no NOEs were detected between the two groups (morpholine ring and ethyl chain) bound to the sydnone moiety, both in the free state of molsidomine and in its bound forms, therefore the drug must have an extended structure in agreement with the MACROMODEL (version 8.1)[14a–c] conformational search using an ATM line ad hoc modified water.slv file. The crystallographic, aqueous and in vacuo optimized structure fits each other very well starting from both the above X-ray and a de novo built structures, that is, no changes were observed. As described above, it is noteworthy that the best fitting aqueous conformer is located above the minimum.

The influence of the crystallization solvent is not trivial (the problems related to polymorphisms and solvated structures). Therefore, this might not be a direct relationship between the stability of a crystal obtained from water and its conformation in solution (e.g., D_2O-NMR). If the compound is hydrophobic, then the water structure may not be so very important for biology, but in this case it is very important and suggests two attach points for the polar groups in the external part of the cyclodextrins.

With respect to the *dry* (computational in vacuo) comparison, it must be also considered that water can have a huge effect especially with an N-ion, so that the in vacuo results could be completely different by the stronger role of effects of electrostatics in charged solutes where the free energies of aqueous solvation can be very large. Comparing with the in vacuo is justified as a kind of validation, and because the subject molecule is rather small and quite rigid, so the lowest energy conformation might be the same in the gas and solvated phases. Moreover, assuming the overall gradient of convergence is less than 0.05 kJ/Åmol (see Section 4), then it is safe to say that the forcefield predicts that the conformation is a minimum. It is a good rule of counterchecking by other approaches and never a priori considering a crystal structure as an absolute energy minimum, as there are always packing constraints which might hamper the molecule from crossing energetic barriers and therefore entrapping the molecule in false minima. These conformations however often correspond to stable calculated geometries. Taken together, all the data by different wet (NMR-crystallography) and dry (computational) sources are in agreement and support the NMR result.

All the calculated in vacuo RMSD values using the CSD retrieved structure as the template (CSD version 5.25, November 2003; Data update 3: July 2004. Code: KABZES)[11a–c,12a,b] fall within very low values (vide infra). Excluding the ethyl fragment from the fit protocol (non-hydrogen atoms superposition), a better RMSD value was found for the *anti* built structure (RMSD 0.287 Å vs. 0.329 Å for the *eclipsed*) with maximum deviation at $C36_{anti}$ and $C35_{eclps}$ morpholine ring (0.491 and 0.691), respectively (Fig. 11). On the contrary, an at all superposition reversed the above trend (0.540 *anti vs.* 0.322 *eclipsed*) with a maximum deviation at $C55_{anti}/_{eclps}$ morpholine ring (1.399 and 0.724), respectively (see Section 4).

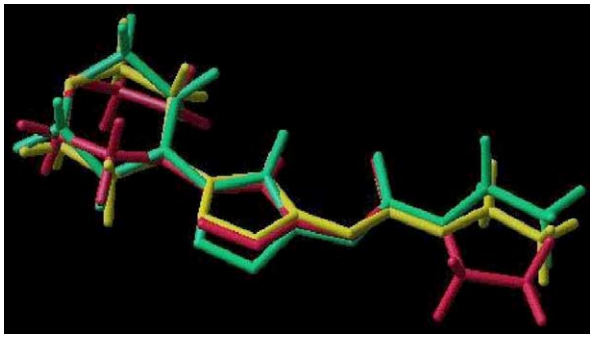

Figure 11. Non-hydrogen atoms superposition of the crystallographic structure (yellow) with the lowest energy conformers in vacuo from the *anti* (fucsia (1)) (RMSD value: 0.287 Å) and *eclipsed* (RMSD value: 0.491 Å) (spring green) starting structure. Similarly it behaved with an in vacuo minimum starting from the X-ray structure. The more distorted morpholine ring and the different orientation (down the molecular plane) of the ethyl fragment are clearly displayed in the conformation from the *anti* (default) starting structure. A conformer in water about 12 kJ above the minimum from an eclipsed built structure behaved similarly to the yellow conformer. See Section 4 for further details. (1) Listed as user 5 in MACROMODEL (version 8.1).[14a,c]

NMR analyses did not define the conformation of morpholine ring in solution, even though the scarce differentiation of pairs of pseudoequatorial and pseudoaxial protons in the NMR spectra allowed us to hypothesize copresence of its boat-chair conformers, rapid exchanging on the NMR time scale. Unfortunately, due to the use of water as solvent, low temperature measurements could not be performed. Therefore, a graphical representation of the stereochemistry of the molsidomine complexes is reported in Figure 12, in which only the chair conformers are depicted. It is noteworthy that the chair conformation of the soft morpholine ring is in agreement with the crystallographic structure and the MACROMODEL (version 8.1)[14a–c] conformational search as implemented in the MAESTRO suite (version 5.1).[14a–c] However the crystal packing might allow space to accommodate also the less populated boat conformation[12a,b] the molecular dynamics by MACROMODEL (version 8.1)[14a–c] did not find boat conformers. SYBYL 6.9[15] scarcely located, respectively, at higher energies (19.92 kcal) with respect to the chair minimum (9.97 kcal) some boat conformers which might be unreliable or artifacts. Both the computational analyses are also in agreement on the strong distortion of the morpholine moiety which is affected by the stiff sydnonimine fragment. A positional change at the H atoms C33 and C35 (Fig. 7) might be a prerequisite for the transition between the two conformations.[12a,12b]

Boat conformations of the morpholine ring were not observed during explicit water simulations by the software AMBER 8.0.[16a–c] The torsion angles O34-C33-C32-N31 and O34-C35-C36-N31 (Fig. 13) shifted between *−gauche* (−60°) and *+gauche* (+60°) after 350, 770, and 850 ps indicating that the ring system was shifting from one chair to another chair conformation during the simulation. The potential energy of the sampled coordinate sets (molsidomine and 725 water molecules) indicated that the relative frequency of coordinate sets with low potential energy was higher when the torsion angle O34-C33-C32-N31 was in the *−gauche* conformation

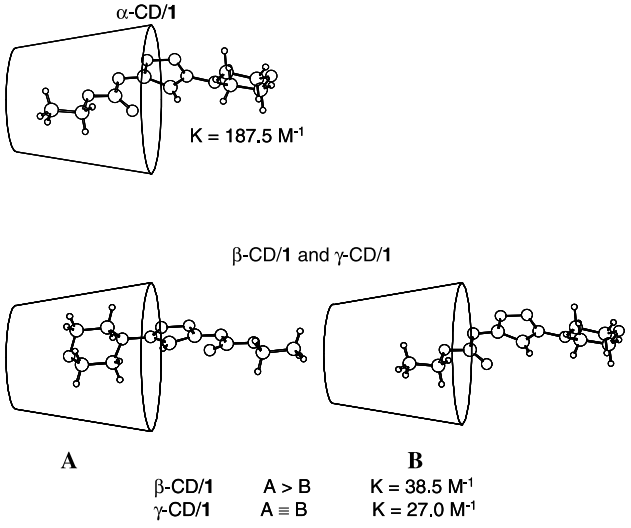

Figure 12. A stereochemical representation of the molsidomine complexes.

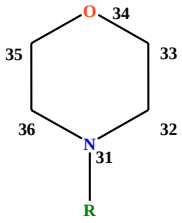

Figure 13. The structure of molsidomine and the investigated torsional angles. **R** stands for the part of the molecule not explicitly considered. Numbering scheme according to Giordano et al.[12a]

(0–350 and 770–850 ps) than in the *+gauche* conformation (350–770 and 850–1000 ps). However, some of the coordinates with the torsion angle O34-C33-C32-N31 in *+gauche* conformation had the potential energy in the same range as those with the O34-C33-C32-N31 torsion angle in *−gauche*, the relative frequency of low energy coordinate sets was much lower during that period (350–770 and 850–1000 ps). In the period when the O34-C33-C32-N31, torsion angle was in *−gauche* (0–350 and 770–850 ps) the molsidomine structure was more similar to the X-ray structure than between 350–770 and 850–1000 ps. After energy minimization of the lowest energy coordinate set (molsidomine and the water molecules) from the periods 0–350 to 770–850 ps the RMSD of molsidomine from the X-ray structure (non-hydrogen atoms) was 0.28 Å. After energy minimization of the lowest energy coordinate set from the periods 350–770 to 850–1000 ps the RMSD from the X-ray structure was 1.0 Å. Based on the relatively short MD simulation, it seems like the molsidomine conformations with the O34-C33-C32-N31 torsion angle in *−gauche*, as in the X-ray structure, are generally energetically more favourable in water than the molsidomine conformation with the torsion angle O34-C35-C36-N31 in *+gauche* conformation. The reason for which the last part of the simulation is most in agreement with experimental data may be the length of the simulation. Most properly, a longer simulation would give most of the molecular system seen during the last part. A quite long period is necessary to scan the conformational space of the system.

Then, we moved forward toward the comprehension of molsidomine complexation phenomena by cyclodextrins, in fact the inclusion proceeded by the large diameter cavity independently on the cavity size (Fig. 12).

This is mainly surprising in the case of γ-CD, which, in principle, could have a favoured inclusion by both the narrower and larger rims. Therefore the driving force of complexation must rely on the attractive interactions between the strongly polar groups of molsidomine, in the area of sydnone ring (Fig. 7), and the secondary hydroxyls lying on the large rim.

2.1.3. Association constants determination. In principle, a good fit between the internal cavity and molsidomine-included moieties could contribute to the stabilization of the inclusion complexes. To go deeply into this matter, we determined the association constants of the three complexes formed in solution. The more common

approach to the association constants determination of fast-exchanging species involves the analysis of the chemical shifts dependence on the concentration of progressively diluted solutions containing the two complexed species or the analysis of the complexation shifts in solutions containing a fixed low amount of one component and increasing excesses of the other. The equation giving the measured chemical shift (δ_{obs}) as weighted average of its value in the complexed (δ_b) and uncomplexed (δ_f) forms (Eq. 1, where X_b is the molar fraction of the bound species) is combined to the equation giving the association constant (Eq. 2, for a 1:1 complexation stoichiometry, where C_0 is the initial concentration of each species), to express the dependence of the observed chemical shift on the solution concentration, in the forms suitable for linear or non-linear fittings.

$$\delta_{obs} = \delta_b X_b + \delta_f(1 - X_b), \tag{1}$$

$$K_a = \frac{X_b}{C_0(1 - X_b)^2}. \tag{2}$$

The procedure is time consuming, as many solutions must be prepared and analyzed. However, in the case of host–guest inclusion complexes, an alternative method can help us, based on the determination of the diffusion coefficients (D) (Eq. 3) by DOSY analyses.[17] The diffusion coefficient depends on the size of the molecule:

$$D = \frac{kT}{6\pi\eta r}, \tag{3}$$

where k is the Boltzmann constant, T is the absolute temperature, η is the dynamic viscosity and r is the radius of the molecule.

The diffusion coefficient observed (D_{obs}) in the NMR experiment (fast-exchange condition) is the weighted average of the diffusion coefficient of bound (D_b) and free (D_f) guest:

$$D_{obs} = X_b D_b + (1 - X_b)D_f. \tag{4}$$

Therefore, the fraction of bound guest can be determined by

$$X_b = \frac{D_{obs} - D_f}{D_b - D_f}. \tag{5}$$

Taking into account that typically the guest molecules are significantly smaller than cyclodextrins, we can assume the diffusion parameter of the bound guest (D_b) being equal to that of the cyclodextrin (D_{host}).[18] It is noteworthy that in these cases, it is possible to obtain directly the molar fraction of the bound guest by employing Eq. 5 and, hence, by using Eq. 2, the association constant by single point determinations.

Therefore, we analyzed the DOSY map of the equimolar mixture molsidomine/α-CD at 20 mM concentration of each component and measured for molsidomine a diffusion coefficient of 4.18×10^{-10} m^2 s (Table 2).

By using Eq. 5 and the diffusion coefficients of the free compounds reported in Table 2, we calculated a molar fraction of bound molsidomine equal to 0.60, which corresponded to an association constant of 188 M^{-1}. As this value has been obtained on the assumption of a 1:1 complexation stoichiometry, we calculated the association constant at a very different concentration (2.4 mM) and the values obtained are reported in Table 2. The association constant by these farther data set was in extraordinary agreement (198 M^{-1}), confirming that our initial assumption can be considered correct. The same procedure applied to β- and γ-CD gave, by single point determinations, association constants of 39 and 27 M^{-1}, respectively, (Table 2), that is, significantly lower with respect to α-CD and very similar to each other. It is noteworthy that, in all cases, the good agreement between the diffusion coefficients of the cyclodextrin in the absence and in the presence of the drug supported the goodness of the introduced approximation.

3. Conclusions

Our results by a combined NMR study and crystallographic data analysis with the support of molecular modelling address toward an important topic regarding the influence of the sydnone structure in the inclusion of the molsidomine into the different cyclodextrins: the relative contribution of attractive interactions occurring at the external surface of the cyclodextrins (involving their hydroxyl functions) and at the internal apolar surfaces. The first can control the selectivity of the inclusion stereochemistry: by the large cavity versus the small cavity inclusion. But a good fit between cavity size and included systems, essential to optimize the attractive hydrophobic interactions, is the basis of the stabilization of the included molecules. Overall, the depicted dynamic process of binding between the cyclodextrin and the mesoionic guest results from a subtle interplay between polar and steric conditions, the hydration of the free species and the complexes, van der Waals interactions, dipole–dipole interactions, hydrogen bonding and mutual conformational changes of the interacting molecules. The complexation is controlled by topological and topographic

Table 2. Diffusion coefficients (D) of cyclodextrins and **1** in mixtures (D^{obs}) and in the free state (D^{free}), molar fraction of bound **1** and association constants

	Total C (mM)	D^{free}_{host} (m^2s)	D^{free}_1 (m^2s)	D^{obs}_1 (m^2s)	X_b	K (M^{-1})
α-CD/**1**	40	2.94×10^{-10}	6.00×10^{-10}	4.18×10^{-10}	0.60	187.5
α-CD/**1**	4.8	2.94×10^{-10}	6.00×10^{-10}	5.20×10^{-10}	0.26	197.8
β-CD/**1**	31.8	2.73×10^{-10}	6.00×10^{-10}	5.01×10^{-10}	0.30	38.5
γ-CD/**1**	40	2.36×10^{-10}	6.00×10^{-10}	4.97×10^{-10}	0.28	27.0

parameters, indicating the relevance of the van der Waals and hydrophobic interactions.[14c] An analysis of the CSD structure reveals a strong tendency of the molsidomine to form such kind of contacts (Fig. 7).

Molsidomine represents an ideal model to exemplify the cavity selectivity: it is constituted by a central polar ring, the sydnone moiety, flanked by two less polar groups having different sizes, the smaller ethyl chain and the larger morpholine ring. Its polar heart drives always toward the interaction with the secondary hydroxyls, leading both groups in proximity of the large diameter cavity; however, a good fit between cavity size and included moieties is given by α-CD toward the ethyl group, thus leading to a high degree of stabilization. By contrast, the cavities of β- and γ-CD are too large to give a good fit both with the two moieties, that is, ethyl group and morpholine ring; therefore these are included with low selectivity and the stabilizing contribution relies only on the superficial interactions which are similar for both complexes. Therefore, including the drug into the three cyclodextrins might present the potential to modulate its bioavailabity and therefore to catch-up with different therapeutic needs.

4. Experimental

4.1. General methods

All NMR spectra in D_2O were recorded on a Varian INOVA600 spectrometer operating at 600 MHz for ^1H, using a 5 mm broadband inverse probe with *z*-axis gradient. The sample temperature was maintained at 25 °C. The 2D NMR spectra were obtained by using standard sequences. Proton gCOSY 2D spectra were recorded in the absolute mode acquiring 8 scans with a 3 s relaxation delay between acquisitions for each of 512 FIDs. Proton 1D ROESY spectra were recorded using selective pulses generated by means of the Varian Pandora Software. The selective 1D ROESY spectra were acquired with 1024 scans in 32 K data points with a 3 s relaxation delay and a mixing time of 1.2 s. DOSY experiments were carried out by using a simulated echo sequence with self-compensating gradient schemes, a spectral width of 6093 Hz and 64 K data points. Typically, a value of 400 ms was used for Δ, 1.0 ms for δ and g was varied in 30 steps (16 transients each) to obtain an approximately 90–95% decrease in the resonance intensity at the largest gradient amplitudes. Tha baselines of all arrayed spectra were corrected prior to processing the data. After data acquisition, each FID was apodized with 3.0 Hz line broadening and Fourier-transformed. The data were processed with the DOSY macro (involving the determination of the resonance heights of all the signals above a pre-established threshold and the fitting of the decay curve for each resonance to a Gaussian function) to obtain pseudo two-dimensional spectra with NMR chemical shifts along one axis, and calculated diffusion coefficients along the other.

The molsidomine structure (CSD code: KABZES)[12a,b] was retrieved from the Cambridge Structural Database (CSD) (version 5.25, November 2003. Data update 3: July 2004) by the software CONQUEST (version 1.6)[11a–c] and the crystal structure visualization and analysis were carried out by the software Mercury (version 1.2.1).[11b,c] All the CSD protocols were run on a PC working under WINDOWS XP. The Contacts functionality as in MERCURY was used to find the key intermolecular interactions in a crystal structure and the main features of the crystal packing (Fig. 7).

All the modelling studies were carried out on a SGI-OCTANE and R5000 O2 workstations operating under IRIX 6.5.+ using the softwares MACROMODEL (version 8.1) as implemented in the version 5.1 of the MAESTRO suite[14a,b] and SYBYL.[15]

The AMBER 8.0 program package[16a–c] running on a HP Superdome[‡] was used for molecular dynamics simulation of molsidomine as .pdb. The simulation of molsidomine was performed for 1000 ps at the default temperature of 310 K (37 °C) in a box of water molecules. The coordinate sets were sampled every 0.5 ps, giving a total of 2000 coordinate sets during the simulation. The size of the water box was: 38.8Å × 30.2Å × 30.2 Å, a total of 725 water molecules. The equilibrium is included in the 1000 ps and is very fast for such a small system. The first 30–50 ps might be considered equilibrium which is enough when we have an energetically stable system, that is, the relationship between potential and kinetic energy is stable.

The CSD file was first exported to .pdb then saved as .prj (for MACROMODEL)[14a,b] or mol2 for SYBYL.[15] The atom potential types bond orders were carefully checked to evaluate their correctness with respect to the intended structure prior the modelling conformational session. The lack of bond order records in the PDB format necessitates that this step be diligently performed.

Considering the influence a possible wrong starting structure might have on the final result of a conformational analysis, the aqueous and in vacuo results from the crystallographic structure (see above) were further checked by a conformational running from a de novo built structure. It must be considered that, overall, the building of the molecule and the final minima seems to be affected because of the size of the fragments selected from the MAESTRO 5.1 library.[14a,b]

[‡] The HP Superdome is a part of the supercomputing facilities in Norway and uses the superscalar HP PA-RISC processor, capable of 4 instructions per cycle. Adding it up, the theoretical peak performance of Nana is 71 GFlops. The Superdome has a hierarchical structure with processors, cells and ccNUMA systems being the basic building blocks. Cache-coherent non-uniform memory access (ccNUMA) provides the capabilities that any processor on any node can directly address any byte of memory on any node, by processor issued load or store instructions. Cache coherence is maintained by a directory-based coherence scheme where each cache-line in the memory systems is expanded by a set of tab-bits, which are set and used by the hardware and the operating system.

Provided that no conceptual differences are in the final results, different building procedures can slightly affect in terms of shape the final conformation, and the building step necessitates to be diligently performed and counterchecked by different starting structures[§]. Using the amide fragment (N → C) from the pulldown menu as implemented in the version 5.1 of the MAESTRO suite library[14a,b] with the default *anti* option *on* in the JOINING GEOMETRY menu of the build panel window when the exocyclic –N → ester fragment is built, an eclipsed geometry which is similar to the crystal was obtained.

Aqueous and in vacuo conformational analyses and molecular dynamics (MD) with simulated annealing by MACROMODEL[14a–c] were performed using the Monte Carlo Multiple Minimum (MCMM) Search protocol with the MMFFs. The water.slv file in the GB/SA was ad hoc modified in the ATM line with the anionic sp^3 $N^{(-)}$ parameters to allow the aqueous optimization (see also the Acknowledgment section). Although these parameters are not actually validated, yet they seem quite reliable. In the Monte Carlo approach, the dynamics of a molecule is simulated by randomly changing dihedral angle rotations or atom positions. Then, the trial conformation is accepted if its energy has decreased from the previous one. If the energy is higher, there are various criteria to select or not the calculated conformer. In our simulations, all of the dihedral angles of single linear bonds were also allowed to move freely using the TORS command (atoms 13–15 and the whole molecule) instead of the TORC which is assigned as a default in amides and puts limits on the values of the torsions around N–C bonds. The conformation was accepted if the energy was lower than that of the previous conformation or within a fixed energy window (20 kJ mol^{-1}) as selector. Comparative conformational analyses including the two bound waters as in the X-ray structure were also carried out with the MOLS (the two water molecules can globally translate/rotate in the search) or ATOM FREEZE commands *on*.

Prior to submitting the ligands to the search protocol, a minimization was carried out using the Merck Molecular Force Fields (MMFFs) as implemented in MACROMODEL (version 8.1),[14a–c] where the MMFF is the default one. MMFF*s* is preferable for small charged ligands. The lowest energy conformers were further minimized. Generally, all the minimizations were performed as above reported. Default options were used with the Polak–Ribiere Conjugate Gradient (PRCG) scheme, until a gradient of 0.001 kJ/Åmol was reached. To search the conformational space, 5000MC steps were performed on each starting conformation. Least squares superposition of all non-hydrogen atoms was used to eliminate duplicate conformations. An energy cut-off of 20.0 kJ mol^{-1}, high enough to map the conformational space, including the bioactive conformation, was applied to the search results. The eight lowest energy conformers (the conformers showed energy values in the same range) in vacuo from the CSD retrieved (version 5.25, November 2003. Data update 3: July 2004. Code: KABZES)[11a–c] and the de novo built structures within ~8 kJ mol^{-1} were further optimized using the multiple minimization protocol as implemented in the software MACROMODEL (version 8.1).[14a–c] Higher energy values were generally obtained for the conformers from the *anti* built structure. Default parameters were used except for a lower convergence criteria (0.001). The superpose option as in the software MACROMODEL (version 8.1)[14a–c] (non-hydrogen superposition) was used to calculate the root mean square distance (RMSD) values (Å) between the crystallographic conformation overall assumed as an energy minimum (see above) and the computational lowest energy conformers in vacuo (Fig. 11) (E_{eclips} = 70.475 kJ mol^{-1}; E_{anti} = 97.974 kJ mol^{-1}). The overestimations of the energy values is an artifact due to the missing water effect (vide infra) on the charged structure of the molsidomine.

Molecular dynamics (MD) by MACROMODEL[14a–c] (simulation T: 300 K with annealing at 20 K , time steps: 1.5 fs, equilibration time: ps 10, simulation time (ps) 40)were carried out using the EXNB option. Extended cut-off distances are, 8 Å in vdW, 20Å in charge/charge electrostatics. Standard defaults in the absence of this command are 7Å for vdW and 12Å for charge/charge electrostatics. Other cut-offs may be selected by adding values for arg5–8. Calculations dealing with ions should use the EXNB option.

Large distance values for cut-offs generally slow calculations, but often make convergence smoother. Occasional problems with energies and gradients which appear to increase upon repeated minimizations may usually be solved by using long van der Waals and electrostatic cut-off distances. The MM2/MM3 and MMFF force fields use complete pair lists (no cut-offs) for van der Waals and electrostatic interactions.

The SYBYL (version 6.9)[15] Molecular Dynamics with simulated annealing was carried out using the TRIPOS Force Field (100 cycles, 2000–0°K/1000 fs (default) with 'minimize before annealing' option on.

The FIT protocol as implemented in SYBYL (version 6.9)[15] was used to compare the different conformers.

[§] In the light of the issues on the molsidomine building described in this manuscript we decided to re-examine the building mode of a structure which was the subject of a previously published study.[14c] Using a *step by step* joining of single fragments [phenyl–carbonyl–amine–amine-carbonyl] the 'GROW' option (with all the other options as default) as in the MAESTRO suite (version 5.1)[14a,b] was selected to have a direct *anti* building of the CONHNHCO carbohydrazide fragment. The previously reported protocol using big fragments without the GROW[14c] option gave a starting structure with *cis* oxygens due to the subjectively substitued H atom in the first $CONH_2$ fragment by that NHCO. The GROW approach gave *trans* oxygens in the CONHNHCO moiety of the structure. Besides a perfect conceptual agreement with the NMR results (as it already was for the results in the published paper)[14c] a much better fit between the NMR and the computational conformations was found (MMFFs). The building mode, that is, the starting structure can affect (based on our experience not conceptually) but more or less in the shape (energy values ranges quite similarly) the final calculated conformation.

4.2. Materials

The α-, β- and γ-cyclodextrins were purchased from Fluka. Pure molsidomine was obtained by Et_2O extraction from commercial tablets (MOLSIDAIN, AVENTIS PHARMA). Eighty four tablets were crushed, added to 50 ml of ethyl ether and the flask was kept to shake for 30 min. The insoluble residue was four times extracted. The extracts were pooled and rotary evaporated to give 317 mg of molsidomine characterized by elemental analysis and ^1H NMR. Microanalysis of vacuum-dried sample of molsidomine was obtained on a Carlo Erba 1106 elemental analyzer (over P_2O_5 at 1–2 mmHg, 24 h at 60–80 °C). Results are within 0.4% of theoretical values ($C_9H_{14}N_4O_4$: calcd. C, 44.62; H, 5.83; N, 23.13. Found: C, 44.68; H, 5.89; N, 23.01).

Acknowledgments

The work was supported by the University of Pisa, MIUR (Project 'Engineering of separation systems, sensors and arrays based on chemo- and stereoselective molecular recognition' Grant 2003039537) and ICCOM-CNR. Schrodinger, Inc.[14b] is gratefully acknowledged for the anionic sp^3 $N^{(-)}$ parameters to modify the ATM line of the water.slv file. The above parameters are implemented in the latest release (8.6) of MACROMODEL.[14a,b] Dr. Joseph M. Hayes, Anterio Consult & Research GmbH, Mannheim (Germany) is gratefully acknowledged for the helpful discussion and suggestions for the RC's graduation thesis provided. The Authors thank Prof. Ingebrigt Sylte and Dr. Osman A.B.S.M. Gani, Department of Pharmacology, Institute of Medical Biology, University of Tromsø, Norway for access to the HP Superdome and the helpful suggestions on the AMBER 8.0 program.[16a–c]

References and notes

1. (a) WHO World Health Report, 2003; (b) WHO news release. <www.who.int/mediacentre/releases/2003/pr72/en/./>
2. (a) Megson, I. L. *Drugs Future* **2000**, *7*, 701–715; (b) Wang, P. G.; Xian, M.; Tang, X.; Wu, X.; Wen, Z.; Cai, T.; Janczuk, A. J. *Chem. Rev.* **2002**, *102*, 1091–1134 (and references cited therein)..
3. Maragos, C. M.; Morley, D.; Wink, D. A.; Dunams, T. M.; Saavedra, J. E.; Hoffman, A.; Bove, A. A.; Isaac, L.; Hrabie, J. A.; Larry, K.; Keefer, L. K. *J. Med. Chem.* **1991**, *34*, 3242–3247 (and references cited therein)..
4. Kerwin, J. F., Jr.; Lancaster, J. R., Jr.; Feldman, P. L. *J. Med. Chem.* **1995**, *40*, 4343–4362 (and references cited therein).
5. Artz, J. D.; Toader, V.; Zavorin, S. I.; Bennett, B. M.; Thatcher, G. R. J. *Biochemistry* **2001**, *40*, 9256–9264.
6. Andersen, C. U.; Mulvany, M. J.; Simonsen, U. *Eur. J. Pharmacol.* **2005**, *510*, 87–96 (and references cited therein).
7. Chrysselis, M. C.; Rekka, E. A.; Siskou, I. C.; Kourounakis, P. N. *J. Med. Chem.* **2002**, *45*, 5406–5409.
8. Feelisch, M.; Ostrowski, J.; Noack, E. *J. Cardiovasc. Pharmacol.* **1989**, *14*, S13–S22.
9. (a) Uekama, K.; Horikawa, T.; Yamanaka, M.; Hirayama, F. *J. Pharm. Pharmacol.* **1994**, *46*, 714–717; (b) Hirayama, F.; Yamanaka, M.; Horikawa, T.; Uekama, K. *Chem. Pharm. Bull.* **1995**, *43*, 130–136.
10. Atwood, J. L.; Davies, J. E. D.; Macnicol, D. D.; Vögtle, F. *Comprehensive Supramolecular Chemistry*; Pergamon Press: UK, 1996; Vol. 3.
11. (a) Allen, F. H. *Acta Crystallogr.* **2002**, *B58*, 380–388; (b) Bruno, I. J.; Cole, J. C.; Edgington, P. R.; Kessler, M.; Macrae, C. F.; McCabe, P.; Pearson, J.; Taylor, R. *Acta Crystallogr.* **2002**, *B58*, 389–397; (c) Allen, F. H.; Motherwell, W. D. S. *Acta Crystallogr.* **2002**, *B58*, 407–422.
12. (a) Giordano, F. *Gazz. Chim. Ital.* **1988**, *118*, 501–505; (b) Santoro, F.; Barbier, C.; Giordano, F.; Del Re, G. *J. Mol. Struct. (Theochem)* **1998**, *433*, 291–299.
13. Gringauz, A. *Introduction to Medicinal Chemistry: How Drugs Act and Why*; WILEY-VCH: USA, 1997, 12.7 599–603..
14. (a) Mohamadi, F.; Richards, N. G. J.; Guida, W. C.; Liskamp, R.; Lipton, M.; Caufield, C.; Chang, G.; Hendrickson, T.; Still, W. C. *J. Comput. Chem.* **1990**, *11*, 440–467; (b) Schrodinger, Inc.: 1500 S. W. First Avenue, Suite 1180, Portland OR 97201, USA/One Exchange Place, Suite 604, Jersey City, NJ 07302, US (www.schrodinger.com); (c) Uccello-Barretta, G.; Balzano, F.; Sicoli, G.; Fríglola, C.; Aldana, I.; Monge, A.; Paolino, D.; Guccione, S. *Bioorg. Med. Chem.* **2004**, *12*, 447–458 (and references cited therein).
15. SYBYL Molecular Modelling Software, version 6.8 and 6.9; Tripos Inc.: 1699 S-Hanley Rd, Suite 303, St. Louis, MO 63144-2913, USA (www.tripos.com).
16. (a) Case D. A.; Darden T. A.; Cheatham, T. E., III.; Simmerling, C. L.; Wang, J.; Duke, R. E.; Luo, R.; Merz, K. M.; Wang, B.; Pearlman, D. A.; Crowley, M.; Brozell, S.; Tsui, V.; Gohlke, H.; Mongan, J.; Hornak, V.; Cui, G.; Beroza, P.; Schafmeister, C.; Caldwell, J. W.; Ross, W. S.; Kollman, P. A. **2004** , *AMBER 8*, University of California, San Francisco; (b) Pearlman, D. A.; Case, D. A.; Caldwell, J. W.; Ross, W. S.; Cheatham, T. E., III; DeBolt, S.; Ferguson, D.; Seibel, G.; Kollman, P. *Comput. Phys. Commun.* **1995**, *91*, 1–41; (c) Cornell, W. D.; Cieplak, P.; Bayly, C. I.; Gould, I. R.; Merz, K. M.; Ferguson, D. M.; Spellmeyer, D. C.; Fox, T.; Cadlwell, J. W.; Kollmann, P. A. *J. Am. Chem. Soc* **1995**, *117*, 5179–5197.
17. Johnson, C. S., Jr. *Prog. Nucl. Magn. Reson. Spectrosc.* **1999**, *34*, 203–256.
18. Wimmer, R.; Aachmann, F. L.; Larsen, K. L.; Petersen, S. B. *Carbohydr. Res.* **2002**, *337*, 841–849.